

SINUSOIDAL FREQUENCY ESTIMATION USING FILTER BANKS

Andre Tkacenko and P. P. Vaidyanathan

Dept. of Electrical Engr. 136-93, Caltech, Pasadena, CA 91125, USA
E-mail: andre@systems.caltech.edu, ppvnath@systems.caltech.edu

ABSTRACT

One problem of great interest to the signal processing community is that of estimating the frequencies of sinusoids buried in noise. Traditional methods applied to a fullband signal fail to estimate accurately when the signal-to-noise ratio (SNR) or spacing between frequencies is small. They also fail when the noise is not white and its statistics are unknown. In this paper, we consider these methods when applied to the subbands of a filter bank and show that, through proper choice of analysis filters, the local SNR and frequency spacing increase by the decimation ratio. We also show that the subband noise processes will be, on average, more “white” than the fullband one in terms of the spectral flatness measure. This suggests that if the noise statistics are unknown, there will be less error by estimating in the subbands as opposed to the fullband. Experimental results support this theory, as we shall show.¹

1. INTRODUCTION

The problem of sinusoidal frequency estimation arises in many signal processing applications, most notably array processing. Traditional methods to do this, such as the MUSIC algorithm and the principal components linear prediction (PCLP) method, perform poorly when the SNR and spacing between frequencies is small. In addition, the input noise is assumed white. If this is not the case, colored noise can be accommodated, provided that its statistics are known. However, such statistics may not be known and instead, the noise may be incorrectly assumed white. Such shortcomings lead us to explore new methods to overcome them.

In this paper, we show how to use a digital filter bank to address this problem. With ideal analysis filters and white noise, the local SNR and frequency spacing in the subbands exceed those in the fullband by a factor equal to the decimation ratio. Heuristically, it is clear that if the filters are not ideal but sufficiently suppress spillover between adjacent bands, the above will still hold approximately. Regarding colored noise, we then show, using the spectral flatness measure [7], that for a broad class of analysis banks, the geometric mean of the subband flatness measures is always greater than or equal to the input flatness. This is a generalization of a result given by Rao and Pearlman [4]. It suggests that if the noise statistics are unknown, assuming the noise to be white in the subbands is less harmful than in the fullband. An example is provided which supports this theory.

¹Work supported in parts by the NSF grant MIP 0703755, and by Microsoft Research, Redmond, WA.

1.1. Notations

All notations are as in [5] and [7]. In particular, $(\cdot)^{+(\mathcal{P})}$ denotes the rank \mathcal{P} pseudoinverse of a given matrix, in which only the \mathcal{P} largest singular values are preserved while the rest are set equal to zero. The Fourier transform of $g(Mn)$ is denoted by $[G(e^{j\omega})]_{1M}$.

1.2. Preliminaries

We assume the following discrete time signal model $x(n)$.

$$x(n) = \sum_{i=1}^{\mathcal{P}} A_i s_i(n) + \eta(n), \quad s_i(n) = e^{j\omega_i n}, \quad A_i = |A_i| e^{j\phi_i} \quad (1)$$

Here, \mathcal{P} sinusoidal signals $s_i(n)$, each scaled by the factor A_i , are buried in the complex noise process $\eta(n)$. The goal is to determine the frequencies ω_i given only N_s observations of $x(n)$. The magnitudes $|A_i|$ are unknown but fixed, while the phases ϕ_i are each uniformly distributed over the interval $[-\pi, \pi)$ and pairwise independent. Finally, $\eta(n)$ is a zero mean wide sense stationary (WSS) process uncorrelated with the sinusoids. Traditional methods exploit the special form of the autocorrelation of $x(n)$. From the above assumptions, this sequence is given by,

$$R_{xx}(k) = \sum_{i=1}^{\mathcal{P}} P_i e^{j\omega_i k} + R_{\eta\eta}(k), \quad P_i \triangleq |A_i|^2 \quad (2)$$

Here, P_i denotes the power of the i -th sinusoid. As the PCLP method has been shown experimentally to approach the Cramer-Rao bound for frequency estimation closer than other techniques [2], we will use this method here for estimation in the subbands.

The PCLP Method: Tufts and Kumaresan introduced the PCLP method in 1982, as described in [5]. Here, the ω_i 's in (1) are estimated as peaks of the following pseudospectrum, obtained with $x(n)$'s $N \times N$ autocorrelation matrix, \mathbf{R}_x .

$$\begin{aligned} \widehat{S}_{PCLP}(e^{j\omega}) &= \frac{1}{|A(e^{j\omega})|^2} \\ A(z) &= [1 \quad z^{-1} \quad \dots \quad z^{-(N-1)}] \begin{bmatrix} 1 \\ \widehat{\mathbf{a}} \end{bmatrix} \\ \widehat{\mathbf{a}} &= -\widehat{\mathbf{R}}_x^{+(\mathcal{P})} \mathbf{r}_x, \quad \text{where } \mathbf{R}_x = [\mathbf{r}_x \quad \widehat{\mathbf{R}}_x] \end{aligned}$$

Equivalently, the ω_i 's are estimated as the phases of the roots of the polynomial $A(z)$ closest to the unit circle. Here, we need $N > \mathcal{P}$. One advantage of this method over others is that it has been shown experimentally [5] to be insensitive to an overestimation of \mathcal{P} . This is important, since the exact number of sinusoids in each subband of a filter bank will not be known, even if \mathcal{P} is known.

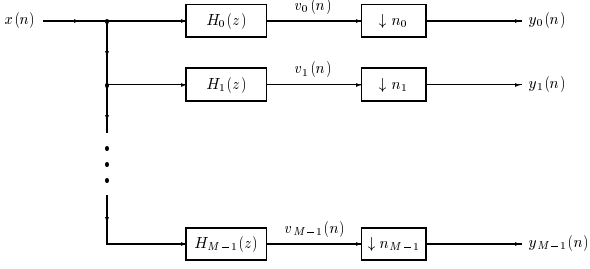


Fig. 1. The M -channel nonuniform analysis bank

2. ANALYSIS OF SUBBAND FREQUENCY ESTIMATION

Suppose that the signal $x(n)$ in (1) is input to the analysis bank shown in Figure 1. For now, assume that the decimation ratios are all equal, i.e. $n_m = M$ for all $0 \leq m \leq M - 1$. Then, the autocorrelation of the subbands signals $y_m(n)$ is given by,

$$R_{y_m y_m}(k) = \sum_{i=1}^P P_i |H_m(e^{j\omega_i})|^2 e^{jM\omega_i k} + R_{\eta_m \eta_m}(k) \quad (3)$$

Here $\eta_m(n)$ denotes the noise process seen in the m -th subband. It can easily be shown that if $[|H_m(e^{j\omega})|^2]_{\downarrow M} = 1$ for all m and the input noise $\eta(n)$ is white with variance σ_η^2 , then $\eta_m(n)$ is also white with variance σ_η^2 . Suppose, for example, that we have,

$$|H_m(e^{j\omega})|^2 = \begin{cases} M, & \omega \in I_m \\ 0, & \text{otherwise} \end{cases}, \quad I_m \triangleq \left[\frac{2\pi m}{M}, \frac{2\pi(m+1)}{M} \right) \quad (4)$$

With this choice of analysis filters, we will soon see that the local SNRs and frequency spacing increase by the decimation ratio M .

2.1. SNR and Frequency Spacing Amplification

With the $|H_m(e^{j\omega})|^2$ as in (4), we have, from (3),

$$\begin{aligned} R_{y_m y_m}(k) &= \sum_{\omega_i \in I_m} M P_i e^{jM\omega_i k} + R_{\eta_m \eta_m}(k) \\ &= \sum_{i=1}^{\mathcal{P}_m} \hat{P}_{i,m} e^{j\hat{\omega}_{i,m} k} + R_{\eta_m \eta_m}(k) \end{aligned} \quad (5)$$

Here \mathcal{P}_m denotes the number of sinusoids present in $y_m(n)$, while $\hat{P}_{i,m} = M P_i$ and $\hat{\omega}_{i,m} = M\omega_i \bmod 2\pi$ denote, respectively, the power and frequency of the i -th sinusoid in the m -th subband, where $\omega_i \in I_m$. If $\eta(n)$ is white with variance σ_η^2 , then we have $R_{\eta_m \eta_m}(k) = R_{\eta \eta}(k) = \sigma_\eta^2 \delta(k)$. Hence, if $\omega_i \in I_m$, the SNR of the i -th sinusoid in the m -th subband is,

$$\text{SNR}_{i,m,\text{sub}} = \frac{\hat{P}_{i,m}}{\sigma_\eta^2} = \frac{M P_i}{\sigma_\eta^2} = M(\text{SNR}_{i,\text{full}})$$

and so the local SNR increases by a factor of M .

If ω_k and ω_l are two frequencies in the interval I_m , then we can express them as,

$$\omega_k = \frac{2\pi m}{M} + \theta_k, \quad \omega_l = \frac{2\pi m}{M} + \theta_l$$

where $0 \leq \theta_k, \theta_l < \frac{2\pi m}{M}$. The spacing between ω_k and ω_l is $\Delta\omega_f \triangleq \omega_k - \omega_l = \theta_k - \theta_l$. As $\hat{\omega}_{i,m} = M\omega_i \bmod 2\pi$, we have $\hat{\omega}_{k,m} = M\theta_k$ and $\hat{\omega}_{l,m} = M\theta_l$, and so the spacing between $\hat{\omega}_{k,m}$ and $\hat{\omega}_{l,m}$ is simply $\Delta\omega_s \triangleq \hat{\omega}_{k,m} - \hat{\omega}_{l,m} = M(\theta_k - \theta_l)$. Hence,

$$\Delta\omega_s = M\Delta\omega_f$$

and so the frequency spacing increases by a factor of M .

With non-ideal analysis filters which are relatively flat in the passband and provide enough attenuation in the stopband, the SNR amplification property will hold approximately, while the increase in frequency spacing will hold exactly.

2.2. Mapping the Subband Frequencies Back to the Fullband

As we desire the fullband frequencies, we need to map the subband frequencies to the fullband ones. If the filters are as in (4), no aliases of the sinusoids appear in more than one subband, and we can map the frequencies as follows.

$$\omega_k = \frac{2\pi m + \hat{\omega}_{i,m}}{M} \text{ for some } k \quad (6)$$

With a sizeable amount of spectral overlap between adjacent analysis filters, an ambiguity exists as to which fullband frequency an observed subband one corresponds. This can be resolved by comparing the size of the peaks of the pseudospectra of the adjacent subbands. The subband whose pseudospectrum is largest at an observed frequency is likely to be the one in which the original fullband sinusoid lies and so we can then use (6) to determine the fullband frequency. If we consider the real analog of the model in (1) and impose that the analysis filters are real-coefficient filters, results analogous to (6) hold but are omitted for sake of brevity.

3. THE WHITENING OF NOISE IN THE SUBBANDS

If $v(n)$ is a WSS process with variance σ_v^2 and power spectral density (psd) $S_{vv}(e^{j\omega})$, then its spectral flatness measure γ_v^2 is defined to be [7],

$$\gamma_v^2 \triangleq \frac{e^{\psi_v}}{\sigma_v^2}, \quad \text{where } \psi_v = \frac{1}{2\pi} \int_{-\pi}^{\pi} \ln S_{vv}(e^{j\omega}) d\omega$$

Throughout this section, suppose that $x(n)$ is any WSS process input to the analysis bank of Figure 1 in which we have,

$$\sum_{i=0}^{M-1} \frac{1}{n_i} = 1, \quad [|H_i(e^{j\omega})|^2]_{\downarrow n_i} = 1 \quad \forall i, \quad \sum_{i=0}^{M-1} \frac{|H_i(e^{j\omega})|^2}{n_i} = 1 \quad \forall \omega \quad (7)$$

Before presenting the main theorem, we first prove two results. For brevity, we define $L \triangleq \text{lcm}\{n_i\}$.

Lemma 1: Geometric mean of the subband variances. We have,

$$\prod_{i=0}^{M-1} (\sigma_{y_i}^2)^{\frac{1}{n_i}} \leq \sigma_x^2,$$

with equality if $S_{xx}(e^{j\omega}) = C(e^{jL\omega})$ for some $C(e^{j\omega}) \geq 0$.

Proof: This is easily proven by using the generalized arithmetic-geometric mean inequality. See (3.36) and (3.40) of [6] for a proof. $\nabla \nabla \nabla$

Theorem 1: Arithmetic mean of the subband quantities

ψ_{y_i} . We have,

$$\sum_{i=0}^{M-1} \frac{1}{n_i} \psi_{y_i} \geq \psi_x,$$

with equality iff $S_{xx}(e^{j\omega}) = C(e^{jL\omega})$ for some $C(e^{jL\omega}) \geq 0$.

Proof: From the log-sum inequality [1], if a_0, \dots, a_{M-1} and b_0, \dots, b_{M-1} are nonnegative numbers and the set $\{a_l\}$ is a probability density function (pdf), then we have,

$$\ln \left(\sum_{l=0}^{M-1} a_l \right) \geq \sum_{l=0}^{M-1} a_l \ln \frac{b_l}{a_l} \quad (8)$$

with equality iff $b_l = K a_l$ for all l and for some $K \geq 0$. As $|H_i(e^{j\omega})|^2|_{n_i} = 1$ for all i from (7), if we define $a_{l,i}$ as $a_{l,i} \triangleq \frac{1}{n_i} \left| H_i \left(e^{j \left(\frac{\omega - 2\pi l}{n_i} \right)} \right) \right|^2$, then $\{a_{l,i}\}$ is a pdf for all i . Thus, as any psd function is nonnegative, for any ω, i , we have, from (8),

$$\begin{aligned} & \ln \left(\frac{1}{n_i} \sum_{l=0}^{n_i-1} S_{v_i v_i} \left(e^{j \left(\frac{\omega - 2\pi l}{n_i} \right)} \right) \right) \\ & \geq \sum_{l=0}^{n_i-1} a_{l,i} \ln \left(\frac{\frac{1}{n_i} S_{v_i v_i} \left(e^{j \left(\frac{\omega - 2\pi l}{n_i} \right)} \right)}{\frac{1}{n_i} \left| H_i \left(e^{j \left(\frac{\omega - 2\pi l}{n_i} \right)} \right) \right|^2} \right) \\ & = \frac{1}{n_i} \sum_{l=0}^{n_i-1} \left| H_i \left(e^{j \left(\frac{\omega - 2\pi l}{n_i} \right)} \right) \right|^2 \ln \left(S_{xx} \left(e^{j \left(\frac{\omega - 2\pi l}{n_i} \right)} \right) \right) \end{aligned} \quad (9)$$

Here, (9) follows from the fact that $S_{v_i v_i}(e^{j\omega}) = |H_i(e^{j\omega})|^2 S_{xx}(e^{j\omega})$ for all ω, i . We have equality above iff $S_{xx}(e^{j\omega})$ is periodic with period $\frac{2\pi}{L}$, which is equivalent to saying that $S_{xx}(e^{j\omega}) = C(e^{jL\omega})$ for some $C(e^{jL\omega}) \geq 0$. From (9), we have,

$$\begin{aligned} \psi_{y_i} &= \frac{1}{2\pi} \int_{-\pi}^{\pi} \ln \left(\frac{1}{n_i} \sum_{l=0}^{n_i-1} S_{v_i v_i} \left(e^{j \left(\frac{\omega - 2\pi l}{n_i} \right)} \right) \right) d\omega \\ &\geq \frac{1}{2\pi n_i} \sum_{l=0}^{n_i-1} \int_{-\pi}^{\pi} \left| H_i \left(e^{j \left(\frac{\omega - 2\pi l}{n_i} \right)} \right) \right|^2 \\ &\quad \times \ln \left(S_{xx} \left(e^{j \left(\frac{\omega - 2\pi l}{n_i} \right)} \right) \right) d\omega \\ &= \frac{1}{2\pi} \sum_{l=0}^{n_i-1} \int_{-\frac{\pi-2\pi l}{n_i}}^{\frac{\pi-2\pi l}{n_i}} |H_i(e^{j\lambda})|^2 \ln(S_{xx}(e^{j\lambda})) d\lambda \\ &= \frac{1}{2\pi} \int_{-\pi}^{\pi} |H_i(e^{j\omega})|^2 \ln(S_{xx}(e^{j\omega})) d\omega \end{aligned} \quad (10)$$

We have equality iff $S_{xx}(e^{j\omega}) = C(e^{jL\omega})$. As (10) is true for all i , we have,

$$\begin{aligned} \sum_{i=0}^{M-1} \frac{1}{n_i} \psi_{y_i} &\geq \frac{1}{2\pi} \int_{-\pi}^{\pi} \left(\sum_{i=0}^{M-1} \frac{|H_i(e^{j\omega})|^2}{n_i} \right) \ln(S_{xx}(e^{j\omega})) d\omega \\ &= \frac{1}{2\pi} \int_{-\pi}^{\pi} \ln(S_{xx}(e^{j\omega})) d\omega = \psi_x \end{aligned} \quad (11)$$

Here, (11) follows from (7). As we have equality iff $S_{xx}(e^{j\omega}) = C(e^{jL\omega})$, this completes the proof.

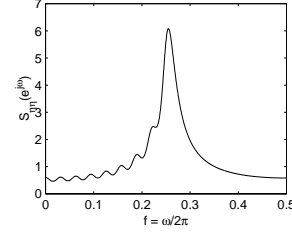


Fig. 2. Input noise power spectrum

▽ ▽ ▽

Combining Lemma 1 and Theorem 1, we have the following theorem. In the next section, an example is given showing how this can be related to the problem of estimating sinusoids in noise.

Theorem 2: Geometric mean of the subband flatness measures. We have,

$$\gamma_y^2 \triangleq \prod_{i=0}^{M-1} (\gamma_{y_i}^2)^{\frac{1}{n_i}} \geq \gamma_x^2$$

with equality if $S_{xx}(e^{j\omega})$ is of the form $S_{xx}(e^{j\omega}) = C(e^{jL\omega})$ for some $C(e^{jL\omega}) \geq 0$.

Proof: We have the following.

$$\gamma_y^2 = \frac{\exp \left(\sum_{i=0}^{M-1} \frac{1}{n_i} \psi_{y_i} \right)}{\prod_{i=0}^{M-1} (\sigma_{y_i}^2)^{\frac{1}{n_i}}} \geq \frac{\exp \left(\sum_{i=0}^{M-1} \frac{1}{n_i} \psi_{y_i} \right)}{\sigma_x^2} \geq \frac{e^{\psi_x}}{\sigma_x^2} = \gamma_x^2 \quad (12)$$

Here, (12) follows from applying Lemma 1, then Theorem 1, and finally the fact that the exponential function is monotonic increasing. As a sufficient condition for equality in (12) is that $S_{xx}(e^{j\omega}) = C(e^{jL\omega})$ for some $C(e^{jL\omega}) \geq 0$, this completes the proof.

▽ ▽ ▽

4. EXPERIMENTAL RESULTS

We will consider here the real analog of the model $x(n)$ given in (1). Suppose that the input $x(n)$ to Figure 1 is given as,

$$x(n) = \sqrt{2} \cos(\omega_1 n + \phi_1) + \sqrt{2} \cos(\omega_2 n + \phi_2) + \eta(n)$$

Here, $\omega_1 = 0.555\pi$ and $\omega_2 = 0.57\pi$, while the noise process $\eta(n)$ is a real ARMA(18,17) process with psd shown in Figure 2. We chose the number of observations to be $N_s = 128$. It should be noted that since the frequency spacing is $\omega_2 - \omega_1 = 0.04712 < \frac{2\pi}{N_s} = 0.04909$, the frequencies can not be estimated from the Fourier transform of the observed signal $x(n)$, as the frequency spacing is below the spectral resolution of the Fourier transform of the finite length observation of $x(n)$.

The analysis bank in Figure 1 used was an 8-channel cosine-modulated filter bank [7] designed using a Kaiser window prototype as described in [3]. The magnitude responses of the filters are shown in Figure 3. With these set of filters, the subband noise flatness measures shown in Table 1 were obtained. The flatness

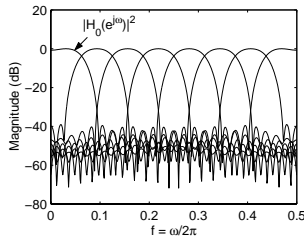


Fig. 3. Magnitude responses of the analysis filters $H_k(z)$

Noise Component	Flatness (γ^2)
Fullband - $\eta(n)$	0.7680
1st Subband	0.9935
2nd Subband	0.9908
3rd Subband	0.9799
4th Subband	0.9039
5th Subband	0.9122
6th Subband	0.9789
7th Subband	0.9949
8th Subband	0.9982
Geometric Mean of Subbands	0.9683

Table 1. Flatness measures of the observed noise processes

of the noise increased noticeably in each subband. In accordance with Theorem 1, the geometric mean of the flatness measures of the subband noise processes exceeds that of the input noise.

PCLP pseudospectra were computed using 50 independent observations of $x(n)$ assuming the input noise to be white. The fullband pseudospectra are shown in Figure 4.

Note that both ω_1 and ω_2 fall within the passband of the 4-th analysis filter. The pseudospectra for this subband are shown in Figure 5. Both the fullband and subband plots indicate the presence of two main peaks. We should mention that the pseudospectra of adjacent subbands also have peaks where those from Figure 5 occur, indicating nonnegligible spectral overlap between the subbands. But as the peaks are strongest in the 4-th subband, we deduce that the fullband sinusoids came from the 4-th subband of the 4-th analysis filter, enabling us to map back the frequencies uniquely.

The mean and standard deviation of the estimates of ω_1 and ω_2 using both methods are shown in Table 2. The subband estimates, when mapped back, were more accurate on average than

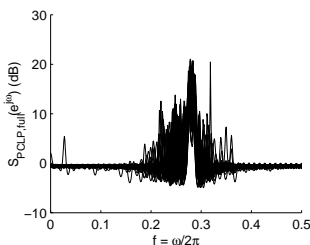


Fig. 4. Fullband pseudospectra

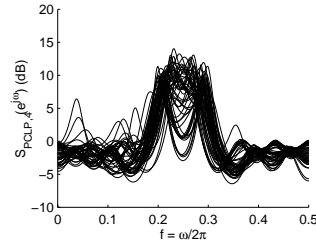


Fig. 5. Pseudospectra of the 4-th subband

Method	$\bar{\omega}_1$ ($\omega_1 = 0.555\pi$)	$\bar{\omega}_2$ ($\omega_2 = 0.57\pi$)	$\sigma_{\bar{\omega}_1}$	$\sigma_{\bar{\omega}_2}$
Fullband	0.5207 π	0.5747 π	0.01501	0.00928
Subband	0.5535 π	0.5708 π	0.000092	0.000098

Table 2. Comparison of fullband and subband methods

the fullband ones. Also, there was less deviation among the subband estimates. Hence, more accuracy was obtained by assuming the noise to be white in the subbands as opposed to in the fullband.

5. CONCLUDING REMARKS

Both the theoretical and practical results presented here reveal advantages to subband frequency estimation. Such benefits do not come without a price. In practice, we only have finite data records. Due to the decimation, fewer observations of the input signal are present in the subbands, which adversely affect the bias and variance of correlation functions estimated there from the observed data. Thus, a tradeoff exists between the number of subband signals and input observations available.

6. REFERENCES

- [1] T. M. Cover and J. A. Thomas, *Elements of Information Theory*, John Wiley & Sons, New York, NY, 1991.
- [2] S. M. Kay, *Modern Spectral Estimation*, Prentice-Hall, Englewood Cliffs, NJ, 1988.
- [3] Y. P. Lin and P. P. Vaidyanathan, "A Kaiser window approach for the design of prototype filters of cosine modulated filterbanks," *IEEE Signal Processing Lett.*, 5(6):132-134, Jun. 1998.
- [4] S. Rao and W. A. Pearlman, "Analysis of Linear Prediction, Coding, and Spectral Estimation from Subbands," *IEEE Trans. Inform. Theory*, 42(4):1160-1178, Jul. 1996.
- [5] C. W. Therrien, *Discrete Random Signals and Statistical Signal Processing*, Prentice-Hall, Englewood Cliffs, NJ, 1992.
- [6] P. P. Vaidyanathan, "Orthonormal and Biorthonormal Filter Banks as Convolver, and Convolutional Coding Gain," *IEEE Trans. Signal Processing*, 41(6):2110-2130, Jun. 1993.
- [7] P. P. Vaidyanathan, *Multirate Systems and Filter Banks*, Prentice-Hall, Englewood Cliffs, NJ, 1993.